Carbohydrate Polymers 111 (2014) 41–46

Contents lists available at ScienceDirect

Carbohydrate Polymers

journal homepage: www.elsevier.com/locate/carbpol

Synthesis and characterization of composite based on cellulose acetate and hydroxyapatite application to the absorption of harmful substances

Khalil Azzaoui[a,*], Abdelatif Lamhamdi[a], El Miloud Mejdoubi[a], Mohammed Berrabah[a], Belkheir Hammouti[b], Abderrahman Elidrissi[b], Moustafa M.G. Fouda[c,**], Salem S. Al-Deyab[c]

[a] Laboratory of Mineral Solid and Analytical Chemistry LMSAC, Department of Chemistry, Faculty of Sciences, Mohamed 1st University, P.O. Box 717, Oujda 60000, Morocco
[b] Laboratory LCAE-URAC18. Faculty of Sciences, Mohamed 1st University, Oujda 60000, Morocco
[c] Petrochemical Research Chair, Department of Chemistry, College of Science, King Saud University, P.O. Box: 2455, Riyadh 11451, Saudi Arabia

ARTICLE INFO

Article history:
Received 9 March 2014
Received in revised form 12 April 2014
Accepted 16 April 2014
Available online 26 April 2014

Keywords:
Composite
Hydroxyapatite
Cellulose acetate
Biomaterials
Bisphenol A (BPA)

ABSTRACT

The aim of this work is to develop composite materials with hydroxyapatite (HAp) mineral and organic matrix such as cellulosic polymers. We use cellulose acetate with different percentages, and then inorganic–organic films were fabricated by evaporation of solvent. The composite films were characterized using emission scanning electron microscopy (FEG-SEM), thermo-gravimetric analysis (TGA) and Fourier transform infra-red (FT-IR) spectra. Test results show that these films are uniform and have good ductility. A strong interaction existed between HAp and cellulosic polymers, and the method allows the production of very fine particles size of about 92 nm. We have developed a new chromatographic method for the quantification of bisphenol A (BPA) in samples of baby food. The result of this study demonstrates how to use this type of composite materials to remove pollutants.

1. Introduction

Recently, composite materials based on calcium phosphate have attracted much attention (Azzaoui, Berrabah, et al., 2013; Azzaoui, Lamhamdi, et al., 2013; Needham, Calafat, & Barr, 2007). Hydroxyapatite is often used as a bone implant material; however, it is used to develop many composites for advanced technologies. Many studies that use bio monitoring used data on food contamination bisphenol A and the environment (Angerer, Ewers, & Wilhelm, 2007; Boogaard, 2007; Calafat, Ye, Silva, Kuklenyik, & Needham, 2006; Needham et al., 2007; Pirkle, Osterloh, Needham, & Sampson, 2005; Yang, Park, & Lee, 2006). This information served as the basis for estimating indirect human exposure to bisphenol A and its potential toxicity. Cellulose acetate is considered one of the essential esters of cellulose. According to the methods used, it can be widely used in different kinds of purposes; such as film formation and membranes. The toxicity of bisphenol A has been extensively studied covering a large range of doses; the study showed adverse effects at doses of 50 mg/kg body weight/day (EU, 2003; Goodman et al., 2006; Gray et al., 2004).

The technology employed for the extraction of BPA from aqueous samples includes solid phase micro-extraction (SPME) (Kasuga et al., 2003), liquid–liquid extraction (LLE) (Deng, Hao, & Wang, 2001) and solid-phase extraction (SPE) (Shafer & Simonian, 2002).

In this work, a novel analytical method based on enrichment and pretreatment of analytes in the water sample CA/HAp sorptive extraction and gas chromatography–mass spectrometry SIM mode have been developed for the rapid analysis of BPA in water. The obtained results demonstrated that CA/HAp/PEG 1000 combined with GC–MS is a simple, rapid and solvent-free method for the analysis of BPA in water.

The aim of this work was then to choose the best stationary phase (TFME) and best chromatographic method for the

* Corresponding author. Tel.: +212 536500603; fax: +212 536500603.
** Corresponding author. Tel.: +966 560773127.
E-mail addresses: k.azzaoui@yahoo.com (K. Azzaoui), mmfoudah@ksu.edu.sa, m_gaballa@yahoo.com (M.M.G. Fouda).

http://dx.doi.org/10.1016/j.carbpol.2014.04.058
0144-8617/

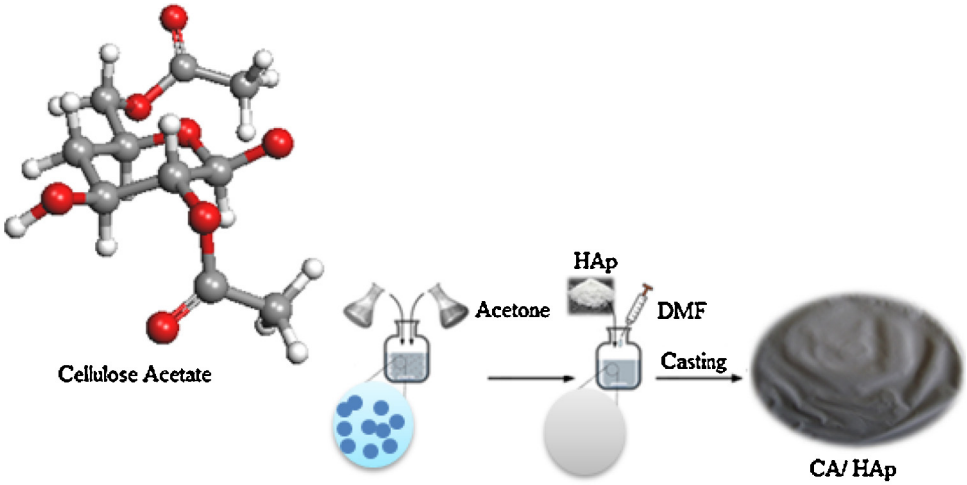

Fig. 1. Schematic representation of synthesis route of composite.

quantification of BPA in samples of baby food matrices, which could be used for routine controls.

2. Experimental and methods

2.1. Materials

Hydroxyapatite (HAp) was synthesized in our laboratory. The cellulose Acetate (CA) (99%), Calcium Nitrate $Ca(NO_3)_2{\cdot}4H_2O$ (99%), Ammonium Hydrogen Phosphate $(NH4)_2{\cdot}HPO_4$ (99%), DMF (Dimethylformamide) and Acetone were purchased from Aldrich. High purity distilled water was used throughout the whole experiment.

2.2. Synthesis of thin film; CA/HAp/PEG1000

The starting substances used in the production of hydroxyapatite were calcium nitrate tetra hydrate and di-ammonium hydrogen phosphate. HAp was produced by following a modified wet chemical method (Azzaoui, Berrabah, et al., 2013; Azzaoui, Lamhamdi, et al., 2013). At 25 °C, 11.76 g of $Ca(NO_3)_2{\cdot}4H_2O$ was first dissolved in a 100 ml volume of water. A solution of 4.06 g $(NH_4)_2{\cdot}HPO_4$ was dissolved in 100 ml volume of water and then added to the $Ca(NO_3)_2{\cdot}4H_2O$ solution over a period of 30 min. The amount of reagents in the solution was calculated to obtain a Ca/P molar ratio value equals 1.67, corresponding to a stoichiometric HAp. About of the polyethylene glycol was added along with the mixture. The pH of the slurry was measured digitally during the precipitation reaction, reaching a final value of pH 10.5.

Cellulose Acetate (CA) polymer were dissolved in acetone at room temperature to form solution A. Solution B was hydroxyapatite (HAp) dispersed in DMF at room temperature and added to solution A. The solution turned to opaque milky white after about half an hour. Thin films were obtained during the procedure with careful temperature control to 50 °C at the temperature rate of 2 °C min^{-1} and maintained for 2 h, and then cleaned in absolute ethanol to remove any possible impurities in the film (Fig. 1).

2.3. Preparation of standards and sample solution

The standard stock solution was prepared by accurately weighing 100 mg of BPA into 1 L (S0) volumetric flask and dissolved in distilled water. The stock solution was diluted with distilled water to obtain solutions S1 and S2, 10 and 1 mg/L, respectively.

Prior to use thin powders were washed with the deionised water, absolute ethanol and dried in the oven at 120 °C for 1 h in order to remove impurities and any possible residual analytes (interferences). Extraction and desorption were carried out as follows: thin powders were immersed in 50 mL of S2 in a glass vial under stirring (contact 20 min), after extraction, the thin powders were taken out from water, gently died with a filter paper and put in an oven to dry at 40 °C for 40 min. finally, the thin s powders were directly placed in centrifuge tube (1.5 ml) to desorb and derive target analyte BPA with BSTFA 1% TMCS (200 μL) under sonication and heated at 70 °C for 30 min. Of the final 0.2 mL final derivative solution, 1 μL was directly injected into the Shimadzu GC/MS system for analysis. In each experiment, the analyte concentration was the same and each solution was analyzed in triplicate.

2.4. Conditions of BPA analysis

For the GC/MS system, a Shimadzu GCMS-QP2010 (Shimadzu, Japan) with GCMS solution 2.5 software was used. The Chromatographic conditions: GC analysis was performed on a Shimadzu QP 2010 system with a fused silica capillary column (30 m, 0.25 mm i.d. and film thickness of 0.25 mm with chemically bonded phase DB-5). The oven temperature was held at 60 °C for 1 min, programmed to rise at 10 °C min^{-1} to 280 °C, and held for 5 min. A sample volume of 0.1–1 μL was injected in splitless mode (high pressure). The injector and interface temperature was kept at 250 °C. Helium was used as the carrier gas. Spectrometric conditions: mass spectrometric parameters: the electron impact ionization energy was 70 eV, the detector voltage 1.7 kV, the ion source temperature was 200 °C and the solvent delay time was 3 min. MS detector was used in multiple ion monitoring mode (ions characteristic of BPA in SIM mode were: m/z = 357 and 372) (Azzaoui, Berrabah, et al., 2013; Azzaoui, Lamhamdi, et al., 2013).

2.5. Physical–chemical characterization

The prepared samples were characterized by making use of Fourier transform infrared spectroscopy (FTIR) using a Schimadzu FT-IR 300 series instrument (Shimadzu Scientific Instruments). FTIR spectra were acquired over the region 400–4000 cm^{-1} in pellet form for 1 mg powder samples mixed with 200 mg spectroscopic grade (KBr). The structure of the samples were evaluated by X-ray diffraction (XRD) using a Rich Siefert 3000 diffractometer (Seifert,

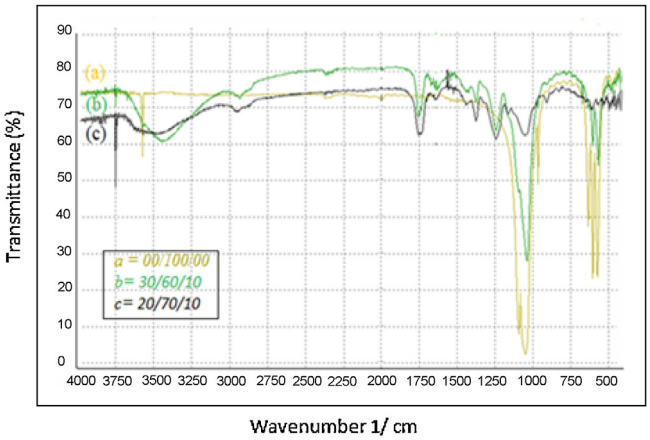

Fig. 2. FTIR spectra of the CA/HAp/PEG 1000 composite, with molar ratios: *a* = 0/100/0, *b* = 30/60/10 and *c* = 20/70/10.

Germany) with Cu-Kα1 radiation (λ = 1.5418 Å). Diffraction peak at 25.9° was selected for determining the crystallite size by Scherrer's formula since it is sharper and isolated from others. This peak allocates to (0 0 2) Miller's plane family and shows the crystal growth along the axis of HAp crystalline structure. The morphology of the materials was analyzed by field emission-scanning electron microscopy (SEM). GC/MS system: A Shimadzu GCMS-QP2010 (Shimadzu, Japan) with GCMS solution 2.5 software.

2.6. Studies in vitro swelling and biodegradable composites

Swelling and biodegradability of composites are studied by immersing the membranes at 37 °C in water and in the biological medium PBS (pH = 7.4). The samples are dried and weighed (W_1). The water absorption (expressed in percentage) was calculated by comparing the initial weight (W_0) with wet weight after swelling (W_1) as shown in Eq. (1).

$$\text{water absorption}(\%) = \frac{W_1 - W_0}{W_0} \times 100 \quad (1)$$

The mass loss was calculated by comparing the initial weight (W_0) with the weight after immersion in the biological medium, and drying at 40 °C for 30 min (W_2) as shown in Eq. (2).

$$\text{weight loss}(\%) = \frac{W_2 - W_0}{W_0} \times 100 \quad (2)$$

3. Results and discussion

3.1. Chemical structure

3.1.1. FTIR analysis

The FTIR spectra of the washed HAp, CA and CA/HAp/PEG 1000 composite as shown in Fig. 2. The bands at 3572 and 632 cm^{-1} belong to the vibration of hydroxyl (O—H) group, the bands at 1089, 1045 and 962 cm^{-1} are the characterization of phosphate stretching vibration and the bands observed at 601, 570 cm^{-1} are owing to the phosphate being in vibration. It is clear from the IR analysis that, the precipitated powders are evidenced to be hydroxyapatite in nature. The presence of polyethylene glycol in hydroxyapatite does not play any role in the structural deformation of hydroxyapatite, meaning that HAp crystallites were prepared. The peak at 3750 cm^{-1} composite CA/HAp/PEG 1000 corresponding to the stretching vibrations of OH groups of cellulose acetate.

The peak at 3572 cm^{-1} is the stretching vibration of the OH group. Compared to the absorption of alcohol group composites (3750 cm^{-1}), alcohol composite graft band appears at a higher

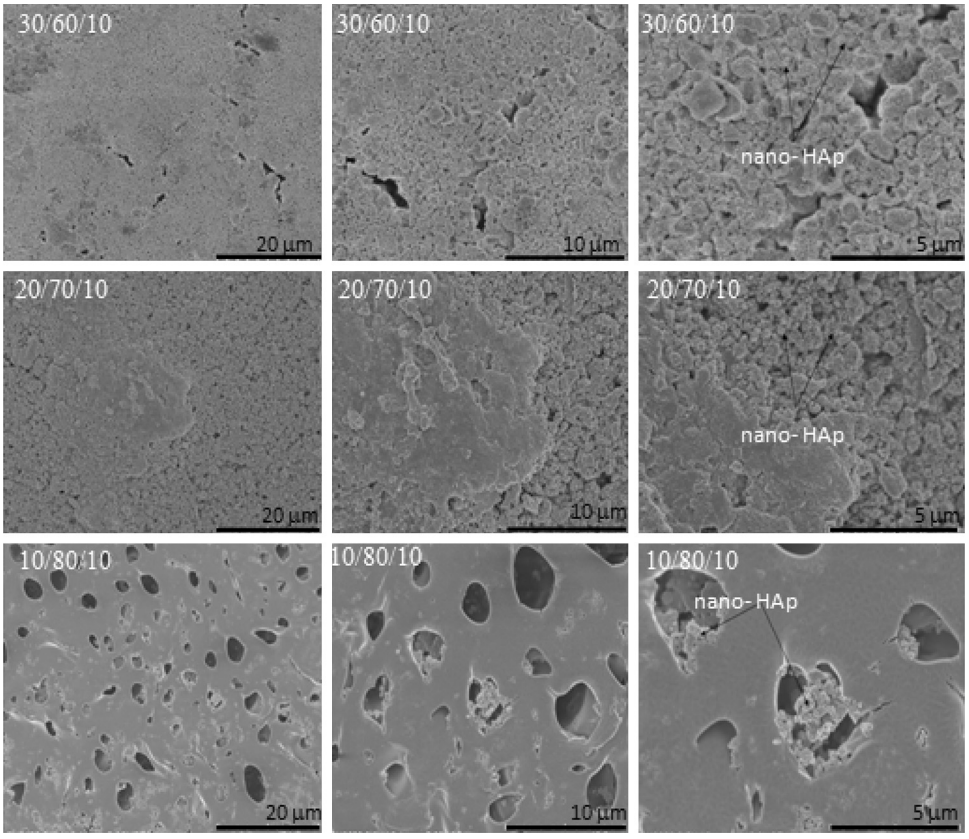

Fig. 3. The SEM/FEG of CA/HAp/PEG 1000 composite scaffold.

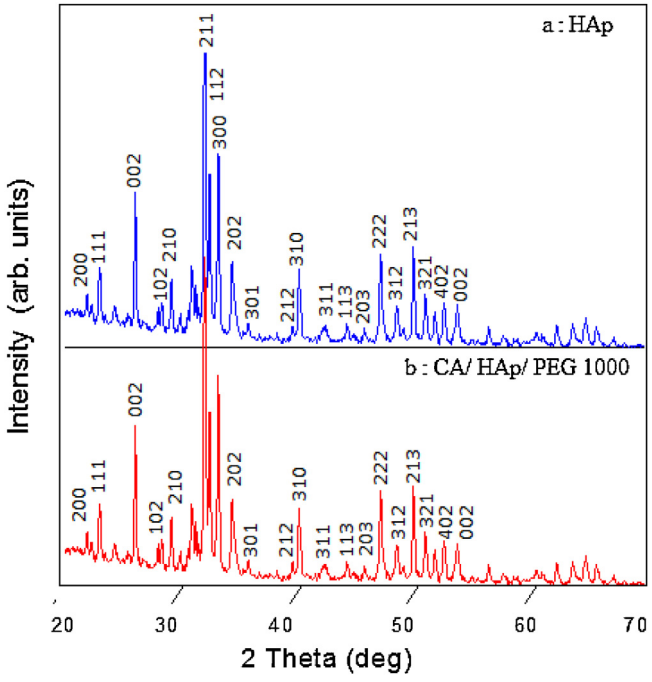

Fig. 4. XRD patterns of HAp and CA/HAp/PEG 1000 composite.

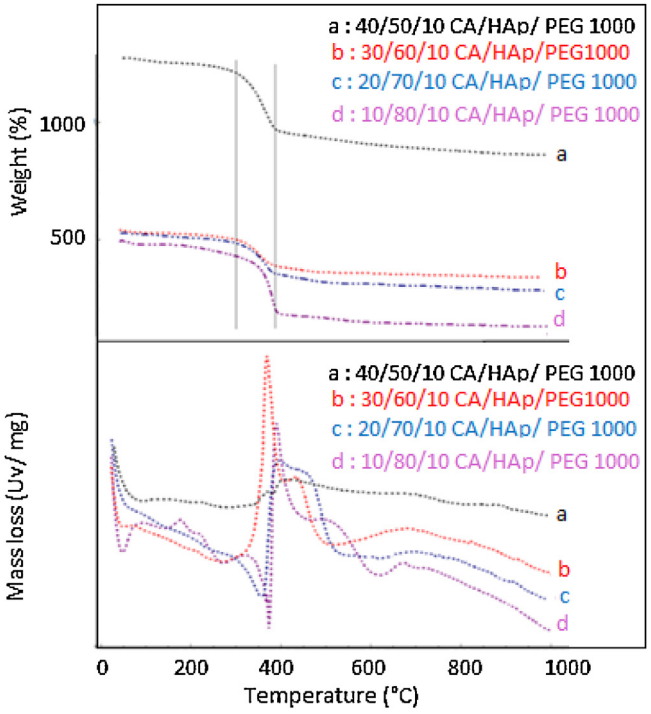

Fig. 5. TGA/DTA curves of: HAp, CA; and CA/HAp/PEG 1000 composite at heating rate 10 °C/min.

frequency. Thus, this result confirms the strong intermolecular interaction of hydrogen bonding between cellulose acetate and treated hydroxyapatite.

Moreover, in order to determine the microstructure of distribution state of n-HAp in composite, SEM/FEG photograph of the CA/HAp/PEG 1000 composite was given (Fig. 3). It shows that HAp crystals are still in the range of nanometer scale and have a good dispersive property in the polymers, which has a positive effect on the mechanical and biological properties of the CA/HAp/PEG 1000 composite scaffold.

SEM images (Fig. 3) disclosed that, the scaffold was three-dimensional complicated irregular porous assembly together with worthy interconnections between the pores, and the walls of the macro pores ranging from 5 to 20 μm contained many micropores.

3.1.2. XRD analysis

The XRD patterns of HAp and CA/HAp/PEG 1000 composite. The patterns designate the presence of well-crystallized hydroxyapatite. The X-ray patterns collected on the powders after heat treatment at 900 °C for 2 h present single phase of HAP. Fig. 4a shows the X-ray patterns of HAP at 900 °C. The X-ray patterns of CA/HAp/PEG 1000 composite at 900 °C are shown in Fig. 4b. These patterns are in good arrangement with the ASTM data (JCPDS) file (no. 09-0432) for hydroxyapatite. No characteristic peaks of impurities, such as calcium hydroxide and calcium phosphates were observed, meaning that phase pure HAp was prepared under the present experimental conditions. The diffraction peaks particularly in the planes (0 0 2), (2 1 1), (1 1 2) and (3 0 0) are high and narrow implying that the HAP crystallizes well.

3.1.3. Thermal properties

Thermo-gravimetric analyses of CA, HAp, and CA/HAp/PEG 1000 composite are presented in Fig. 5. Improvement in thermal stability may be concluded from its thermal analysis curve in Fig. 5. The particles in the network may act as heat barriers therefore, enhance the overall thermal stability of the synthesized composite. All composites have a very similar model, with two stages of weight loss. The first stage is due to water loss, while the second is due to the decomposition of the cellulose acetate. The absences of a step of decomposing the PEG 1000 indicate that the equipment must be removed from the membrane during the phase inversion step. The absence of a step for the decomposition of hydroxyapatite indicates that the treated material is stable. Obviously, the thermal stability of the films increases with the loading of nano/micro-HAp. The film of cellulose acetate is decomposed at about 376.88 °C. For other materials, $a = b$, c and d it was found that the decomposition temperature at 368.67 °C, 355.79 °C and 374.62 °C, respectively. However, the presence of HAp must have induced structural change of the membrane and change the decomposition temperature of this polymer.

3.1.4. Differential scanning calorimetry (DSC)

Fig. 6 shows the different thermal phenomena (observed by differential scanning calorimetry) that occur on/composite CA/HAp/PEG 1000. The glass transition around 92 °C and a melting temperature of the composite around the order of 225 °C. The

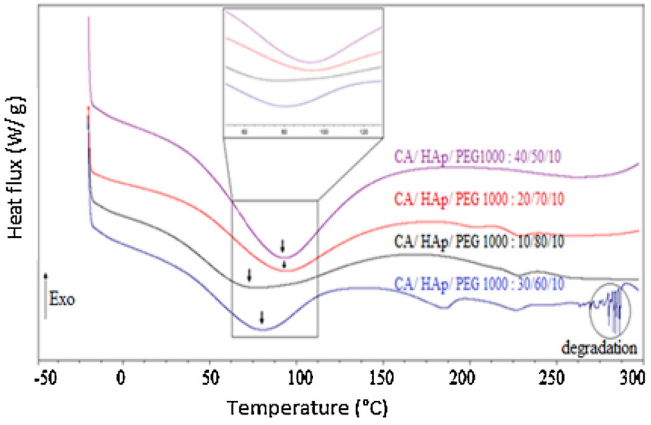

Fig. 6. DSC curves of CA/HAp/PEG 1000 composite.

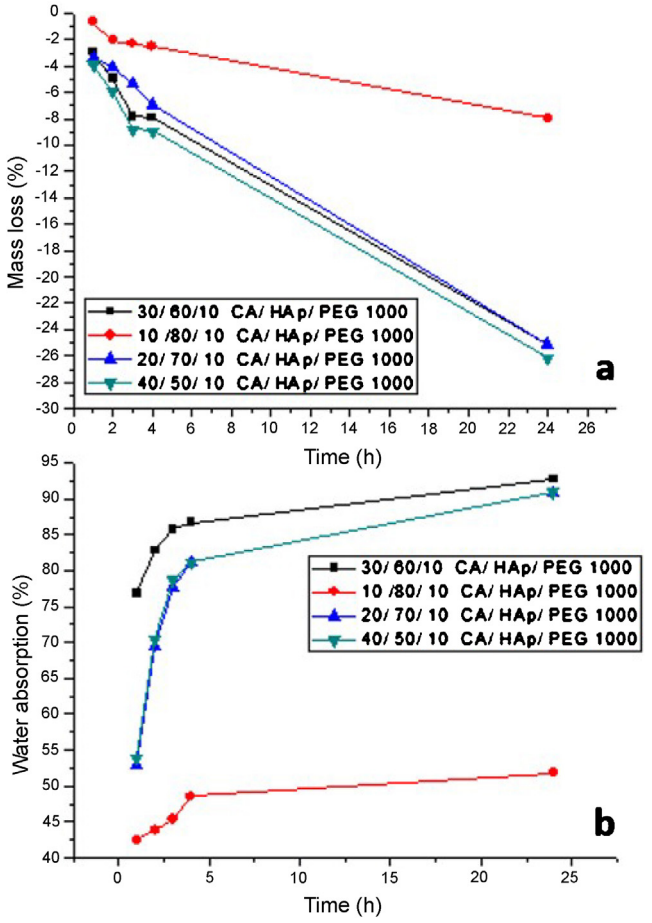

Fig. 7. (a) Biodegradability at 37 °C of membranes CA/HAp/PEG 1000 in PBS, (b) swelling ratio of composite CA/HAp/PEG 1000.

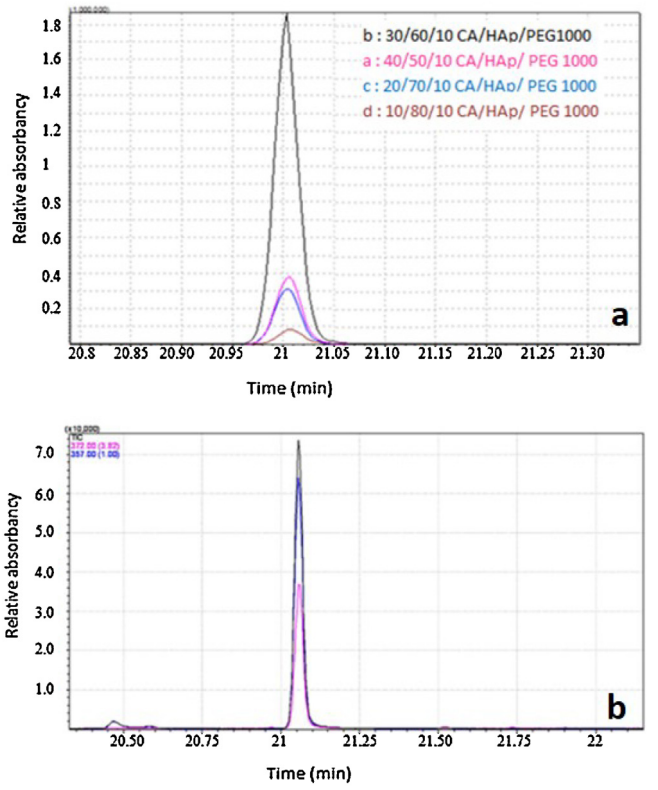

Fig. 8. (a) Chromatogram of BPA desorbed from composites CA/HAp/PEG 1000, (b) chromatograms of BPA desorbed commercial florisil.

endotherms are shifted to higher temperatures when the percentage of treated hydroxyapatite increases, as seen in the case of composite (CA/HAp/PEG 1000): 30/60/10, 20/70/10, 40/50/10, 10/80/10 composite except the endothermic peak at 77.86 °C. Principle the endothermic peak is mainly due to the depolymerization of the cellulose acetate, while the heat is due to a formation of CO_2. The melting peak observed after the composite endothermic decomposition peak is present in all the esters of cellulose, which support the cross-linking reaction occurring during thermal degradation.

3.1.5. Study of swelling and biodegradability in vitro composite CA/HAp/PEG 1000

Fig. 7a shows the biodegradability of membranes CA/HAp/PEG 1000 in PBS solution at pH 7.4 and 37 °C. All samples displayed similar degradation kinetics. Initially, the mass loss of the membrane was almost increases with increasing molar ratios of HAp particles degradation in PBS. This means the surface, not only become coarse, but also porous membrane and permits acceptance of water during degradation. The mass loss of the composite of cellulose acetate/hydroxyapatite treated with increasing immersion time in PBS. After only 1 h of immersion, the maximum loss of mass of the composite CA/HAp/PEG 1000 approximately 4.1% (40/50/10). Time including 4 h undergoes mass loss of immersion up to 7% for the composite (10/80/10), 25% (20/70/10) 25% (30/60/10) and to 25.5% (40/50/10), respectively. Composites loaded with 40% CA lost about 25.5% after 24 h then a slight increase in mass is recorded (Fig. 6).

The initial weight loss is related to the presence at the interface between the particles and the matrix and fissures that will allow the more rapid penetration of water, which will come hydrolyze composite. Fig. 7b shows the swelling kinetics during a 24-hour period, and the swelling of the composite CA/HAp/PEG 1000. Analysis of this figure shows a variation of the swelling ratio for the four composites, 10/80/10 has a swelling ratio while 51% 20/70/10 present a swelling ratio 90%, and the composite with a molar ratio 30/60/10 present a higher rate of inflation (92% at $t = 24$ h). When the percentage varies HAp over the polymer composite swelling augments meaning chains composite absorbs water.

The water absorption and the rate of degradation of the composite materials increase with decrease of HAp.

It is interesting to note that the infrared studies have probably provided additional information on the structural interaction between the components of the composite they were performed using an appropriate technique. These characterization methods, however, may present a useful starting point for further research on the physico-chemical phenomena involved in the type of material studied here.

3.2. Chromatogram of BPA desorbed from the CA/HAp/PEG 1000 composite

The composite CA/HAp/PEG 1000 was characterized by gas chromatography–mass spectrometry (GC–MS), then tested and compared with florisil. The results obtained are shown in (Fig. 8a, b).

The figure shows the evolution of the shape of the chromatographic peak composite adsorbed BPA from water polluted. The best recovery rate of BPA is obtained with the stationary phase 30% and 60% HAp. On the other hand, a low recovery rate for the composite d.

The florisil also leads to very interesting results with recovery rate than that recorded by the composites. This result contributes to the enhancement of composites in the extraction of pollutants.

3.3. Selective binding mechanism

It can be concluded that BPA-composite has a significant discriminating binding capacity for the imprinted BPA in the mixed water. This result demonstrated indirectly that the specific binding sites be existent and is played an important role in the selective binding process. "Hydrogen bonding is an important intramolecular/intermolecular interaction, and it is also a useful adsorption mechanism for adsorptive separation, whereas its directionality and short range confer specific selectivity" as mentioned by (Xu, Zhou, & Huang, 2008). In our experimental, water can also form hydrogen bond to affect the binding capacity, however, the results exhibited that the surface of imprinted adsorbent was hydrophobic. Among interfaces, hydrophobic interactions, van der Waals forces and long range electrostatic interactions are not directional, therefore, they are not considered specific (Bikadi, Demko, & Hazai, 2007). Zhang and Hu (2008) mentioned that the nonspecific adsorption would occur for BPA based on non- covalent synthesis approach as more functional CA/HAp/PEG 1000 are needed during the imprinting synthesis. It was presumed that, hydrogen bonding played substantial role in the selective adsorption process for the specific binding. Zhang and Hu (2008) stated that, specific adsorption would happen selectively for the imprinted molecular by BPA, which could form hydrogen bonds with the carboxyl and carbonyl groups on the binding sites. According to the selective binding outcomes and the surface character of the BPA, the binding pattern of target molecule with CA/HAp/PEG 1000 is engaged. The binding sites confined two specific functional groups, which could rapidly identify BPA molecules through the hydrogen force. Significantly, the dihedral angles of O—H—O were both about 180° resulting in the steadiest affinity for the imprinted BPA binding. Thus, it was realistic to postulate that representation of the double hydrogen-bonding network could present benefits for BPA binding. The distance plot and contact angle of the hydrogen bonding determined the binding stability. In addition, the binding results depicted that, the volume and dimensional structure of the molecular operated as another important role in the BPA binding onto BPA-composite.

4. Conclusion

Synthesis of CA/HAp/PEG 1000 membranes was successfully achieved through dispersion of HAp particles homogeneously in the composite. The composite was characterized by IR and TGA/DTA study, swelling and weight loss shows an interaction between the organic matrix and the HAP matrix by the mean of hydrogen bonding. Morphology showed that the composite has good compatibility between the organic matrix and inorganic matrix (HAp and PLA), the method allows the production of very fine particles size of about 92 nm. Therefore, we can make membranes with well-controlled parameters. The synthesized composites leads to very interesting results with recovery rate of adsorbed BPA from water polluted. This result contributes to the enhancement of composites in the extraction of pollutants.

Acknowledgment

The authors extend their appreciation to the Deanship of Scientific Research at king Saud University for funding the work through the research group project no. RGP-089.

References

Azzaoui, K., Berrabah, M., Mejdoubi, E., Lamhamdi, A., Elidrissi, A., & Hammouti, B. (2013). Use of hydroxylapatite composite membranes for analysis of bisphenol A. *Research on Chemical Intermediates*, http://dx.doi.org/10.1007/s11164-1115-2

Azzaoui, K., Lamhamdi, A., Mejdoubi, E., Berrabah, M., Elidrissi, A., Hammouti, B., et al. (2013). Synthesis of nanostructured hydroxyapatite in presence of polyethylene glycol 1000. *Journal of Chemical and Pharmaceutical Research*, *5*(12), 1209–1216.

Angerer, J., Ewers, U., & Wilhelm, M. (2007). Human biomonitoring, state of the art. *International Journal of Hygiene and Environmental Health*, *210*, 201–228.

Boogaard, P. J. (2007). Human biomonitoring activities—Programmes by industry. *International Journal of Hygiene and Environmental Health*, *210*, 259–261.

Bikadi, Z., Demko, L., & Hazai, E. (2007). Functional and structural characterization of a protein based on analysis of its hydrogen bonding network by hydrogen bonding plot. *Archives of Biochemistry and Biophysics*, *461*(2), 225–234.

Calafat, A. M., Ye, X., Silva, M. J., Kuklenyik, Z., & Needham, L. L. (2006). Human exposure assessment to environmental chemicals using biomonitoring. *International Journal of Andrology*, *29*, 166–171.

Deng, X. M., Hao, J. Y., & Wang, C. S. (2001). *Biomaterials*, *22*, 2867.

EU. (2003). *European Union Risk Assessment Report, Bisphenol A*. Luxembourg: Institute for Health and Consumer Protection, European Chemicals Bureau, European Commission Joint Research Centre, Office for Official Publications of the European Communities., 3rd Priority List, CAS No: 80-05-7.

Goodman, J. E., McConnell, E. E., Sipes, I. G., Witorsch, R. J., Slayton, T. M., Yu, C. J., et al. (2006). An updated weight of the evidence evaluation of reproductive and developmental effects of low doses of bisphenol A. *Critical Reviews in Toxicology*, *36*, 387–457.

Gray, G. M., Cohen, J. T., Cunha, G., Hughes, C., McConnell, E. E., Rhomberg, L., et al. (2004). Weight of the evidence evaluation of low-dose reproductive and development effects of bisphenol A. *Human and Ecological Risk Assessment*, *10*, 875–921.

Kasuga, T., Maeda, H., Kato, K., Nogami, M., Hata, K., & Ueda, M. (2003). *Biomaterials*, *24*, 3247.

Needham, L. L., Calafat, A. M., & Barr, D. B. (2007). Uses and issues of biomonitoring. *International Journal of Hygiene and Environmental Health*, *210*, 229–238.

Pirkle, J. L., Osterloh, J., Needham, L. L., & Sampson, E. J. (2005). National exposure measurements for decisions to protect public health from environmental exposures. *International Journal of Hygiene and Environmental Health*, *208*, 1–5.

Shafer, B. L., & Simonian, P. T. (2002). *Journal of Arthroscopic and Related Surgery*, *18*, 189.

Xu, M. C., Zhou, Y., & Huang, J. H. (2008). Adsorption behaviors of three polymeric adsorbents with amide groups for phenol in aqueous solution. *Journal of Colloid and Interface Science*, *327*(1), 9–14.

Yang, M., Park, M. S., & Lee, H. S. (2006). Endocrine disrupting chemicals: Human exposure and health risks. *Journal of Environmental Science and Health C: Environmental Carcinogenesis & Ecotoxicology Reviews*, *24*, 183–224.

Zhang, Z. B., & Hu, J. Y. (2008). Selective removal of estrogenic compounds by molecular imprinted polymer (MIP). *Water Research*, *42*(15), 4101–4108.